Lasers in Surgery and Medicine 40:323–331 (2008)

In Vivo Real Time Monitoring of Vasoconstriction and Vasodilation by a Combined Diffuse Reflectance Spectroscopy and Doppler Optical Coherence Tomography Approach

A. Douplik,[1,2,3]* D. Morofke,[1,4,5] S. Chiu,[6] V. Bouchelev,[1] L. Mao,[1,7] V.X.D. Yang,[1,5,8] and A. Vitkin[1,6,9]

[1]*Ontario Cancer Institute / Princess Margaret Hospital / University Health Network, Toronto, Canada*
[2]*Xillix Ltd, Toronto, Canada*
[3]*Erlangen Graduate School in Advanced Optical Technologies (SAOT), Friedrich-Alexander Universität Erlangen-Nürnberg, Erlangen, Germany*
[4]*Department of Engineering Science, University of Oxford, Oxford, UK*
[5]*Department of Electrical and Computer Engineering, Ryerson University, Toronto, Canada*
[6]*Department of Medical Biophysics, University of Toronto, Toronto, Canada*
[7]*Institute for Microstructural Sciences, National Research Council Canada, Ottawa, Canada*
[8]*Imaging Research, Sunnybrook Health Science Centre, Toronto, Canada*
[9]*Department of Radiation Oncology, University of Toronto, Toronto, Canada*

Background and Objectives: A combined diffuse reflectance (DR) spectroscopy and doppler optical coherence tomography (DOCT) approach may offer a powerful means for assessment of tissue function, and potentially provide a way for earlier cancer detection through non-invasive local blood supply measurements. The goal of the study was to compare a DR-derived blood-content-related index to a measure of local blood supply flow as furnished by DOCT during manipulations with blood circulation (vasoconstriction and vasodilation), investigate similarities and differences, complementarity of techniques, and then applying these results to the underlying biology.

Study Design/Materials and Methods: Simultaneous DR–DOCT measurements of local blood supply were conducted during drug and mechanically-induced vasoconstriction and vasodilatation on an externalized intact rat gut in vivo. A simple heuristic metric, termed Blood Supply Index was derived from the spectroscopic DR data. This metric variance due to mechanical and pharmacological manipulation of the local blood supply was recorded, and compared with that of two DOCT-derived metrics, namely normalized blood velocity (v_{rel}) and blood vessel diameter (D).

Summary and Conclusions: During vasoconstriction and vasodilatation, the local blood response was successfully visualized by both DOCT and DR metrics and a reproducible correlation was found between these two measurements. A combined DR-DOCT approach may evolve into a technologically-viable method for cross-validation of the derived haemodynamic metrics, yielding a more reliable functional tissue assessment tool for accurate cancer diagnosis and staging. Lasers Surg. Med. 40:323–331, 2008. © 2008 Wiley-Liss, Inc.

Key words: blood supply; hemoglobin; angiogenesis; tumor diagnostics; diffuse reflectance; Doppler optical coherence tomography; spectroscopy; in vivo; vasoconstriction; vasodilatation

INTRODUCTION

Angiogenic changes are a hallmark of many diseases, including cancer [1]. It is assumed that, even in low grade dysplasia, deregulated mitotic processes will require an increased blood supply. This in turn leads to an increase in both vascular density and local hemoglobin concentration within the malignant lesion [2,3]. A practical non-invasive technique would be advantageous for screening local blood supply in hollow organs such as the GI tract due to accessibility challenges and the high tissue motility that can lead to poor measurement reproducibility.

A number of imaging modalities are available for non-invasive studies of blood circulation including Doppler ultrasound [4], laser Doppler flowmetry [5], MR and MR angiography [6], diffusing wave spectroscopy [7,8] and laser scanning confocal imaging [9], among others. Each

Contract grant sponsor: Ontario Research and Development Challenge Fund (ORDCF); Contract grant sponsor: Canadian Institutes for Health Research (CIHR); Contract grant sponsor: Photonics Research Ontario (PRO); Contract grant sponsor: Xillix Technologies Corporation (Richmond, British Columbia, Canada).

*Correspondence to: A. Douplik, Erlangen Graduate School in Advanced Optical Technologies (SAOT), Friedrich-Alexander Universität Erlangen-Nürnberg, Paul-Gordan-Straße 6, 91052 Erlangen, Germany.
E-mail: alexandre.douplik@aot.uni-erlangen.de

Accepted 4 March 2008
Published online in Wiley InterScience (www.interscience.wiley.com).
DOI 10.1002/lsm.20637

method has its own advantages and limitations in terms of the specific circulation-related quantity being measured, complexity, cost, sampling volume, spatial/blood flow resolving ability, suitability for clinical deployment. In this study, we investigate the use of two optical modalities sensitive to vascular changes at the perfusion/microcirculation level, namely diffuse reflectance (DR) and Doppler optical coherence tomography (DOCT).

A combination of DR and DOCT were selected for this study due to, first, their real-time applicability and, second, their sensitivity to vascular changes and tissue perfusion at the microcirculation level. These two imaging modalities are cost effective and easily incorporated into an endoscope or catheter for internal imaging. Through a spectroscopic analysis of wavelength-dependent tissue reflectance signals, the local blood concentration (blood supply) and blood oxygenation can be estimated on a DR system [10]. DOCT is a non-invasive high-resolution imaging modality capable of resolving tissue structure and function with a micrometer resolution and can accurately estimate velocities occurring in vessels ranging from microvascular to aortic [11–13]. The main hypothesis is that both the DR and DOCT derived parameters will reflect local blood supply and thus there will be some correlation between DR and DOCT monitoring results. The goals of the study were to compare a DR-derived blood-content-related index to other measures of local blood supply as furnished by DOCT during manipulations with blood circulation (vasoconstriction and vasodilation), looking for similarities and differences, complimentarity of techniques, and understanding of some underlying biology. Furthermore, this investigation could yield a DR derived empiric parameter sensitive to local blood supply (volume) and less indicative of blood oxygenation that, was sought, can provide a correlation with DOCT-determined parameters which measure the amount and the intensity of blood motion (flow).

Experimental setup was specifically designed to facilitate the closest spatial overlap between the sample volumes of the both methods. A special composite optical probe, enabling both DR and DOCT measurements to be performed over similar interrogated tissue volumes, was developed for this study. DOCT operates in low number of scattering orders, whereas DR operates in multiple scattering (or diffusion) regime. The sampling (catchment) volumes for these techniques are different but due to small source-detector separation for the DR probe (Fig. 1), the sampling volumes for two different techniques are overlapped. Such an overlap in interrogating volume can be achieved only to a partial extent given the geometry and inherent imaging variations between the two modalities.

The local blood supply can be quantified as the ratio of fractional blood volume per volume of tissue (T_{HB}), a

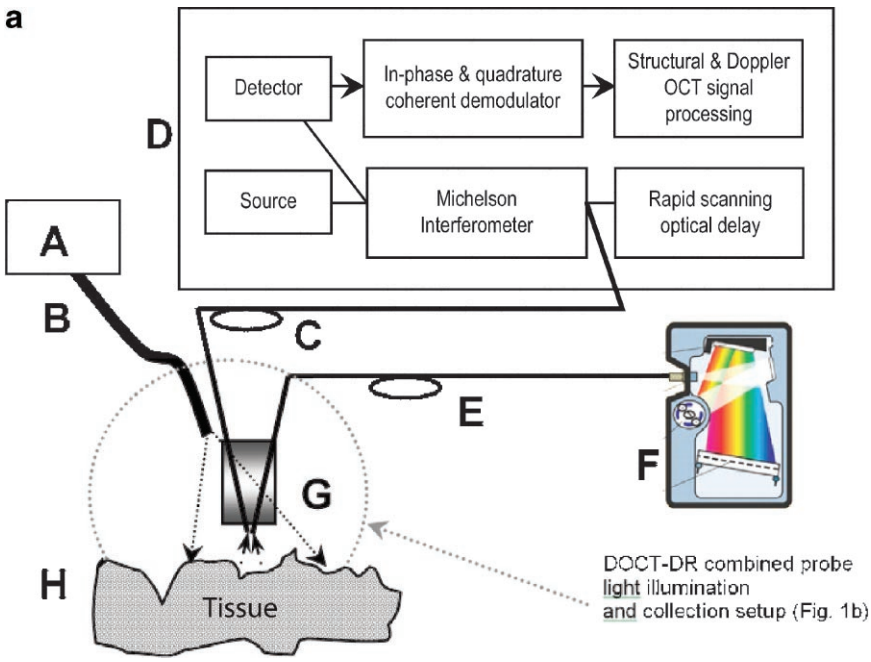

Fig. 1. Schematic diagram of the experimental setup for complementary DR and DOCT measurements in externalized rat colon. **a**: DOCT-DR combined probe light illumination and collection scanning schematic, (**b**) close-up of the combined scanning distal probe, (**c**) photograph of the distal end of the apparatus during externalized rat gut measurements (A). Onco-LIFE® endoscopic light source (Xillix Technologies Corp., Richmond, Canada; high pressure mercury arc lamp, model VIP R 150/P24 qN2, Osram, Germany, 200 mW) (B) Endoscope (Olympus bronchoscope BF Type P40®, power density on tissue surface = 0.050 W/cm^2) (C) DOCT delivery/collection fiber, GRIN lens termination (see subpart b for greater detail) (D) DOCT system (E) DR collection fiber (200 μm core, NA = 0.22) (F) Reflectance spectroscopy system MSL-CS1-USB-VR® (Medspeclab, Inc., Toronto, Canada) (G) Combined reflectance/DOCT fiber probe tip scanning holder (see subpart b for greater detail) (H) Biological tissue (externalized rat gut wall).

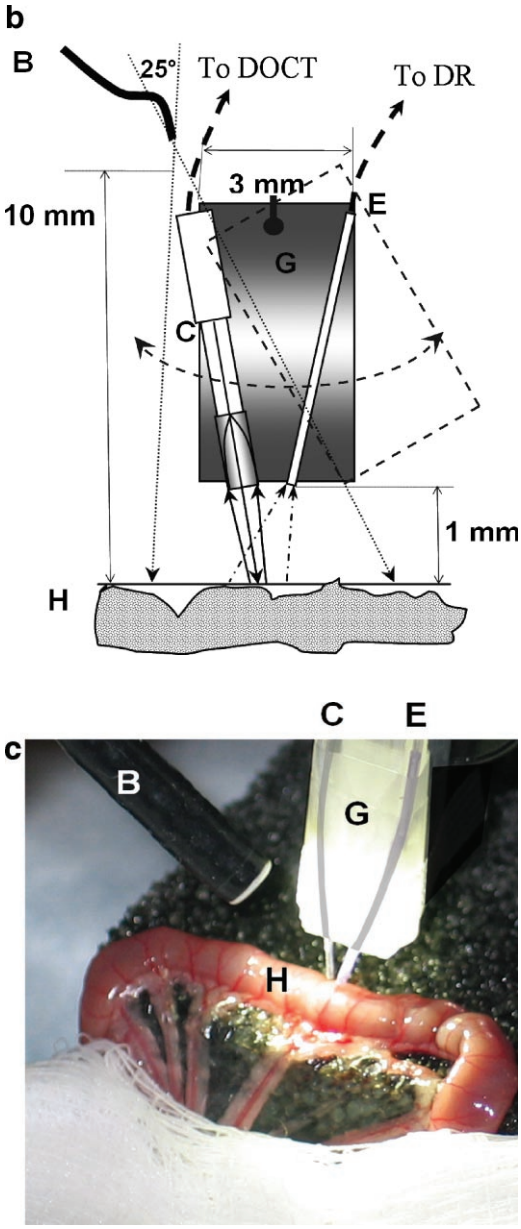

Fig. 1. (*Continued*)

dimensionless quantity with typical values between 0.05 and 0.15 [14,15]. Our literature search revealed two predominant DR-based approaches for estimation of the local blood supply: Toyota et al. derives T_{HB} from the ratio of the reflected green to red light [16], while Stratonnikov and Loschenov [17] implemented a more sophisticated approach using a least square fit to the spectral data. Toyota's method does not account for the local blood supply variation and depends on light collection and the illumination geometry [18,19]. Stratonnikov's approach is more accurate but is computationally intensive making practical real-time implementation difficult. Our DR-based local blood supply estimation method overcomes the shortcomings of the existing models by being robust, computationally efficient, and suitable for real-time analysis.

Similarly, a variety of methods exist for DOCT signal processing and analysis, yielding several blood-flow-related Doppler metrics that can be linked to the biophysical properties of underlying tissue. Further details are available in recent reviews [20–22]. For the purposes of the present study, we selected two DOCT metrics, the normalized blood velocity (v_{rel}) and mean blood vessel diameter (D). These parameters were recorded in response to vasculature changes and correlated with the change in our DR-derived measure of local blood concentration.

This study explores the use of DR and DOCT in an experimental rat model, examining. It represents an initial exploration leading towards the development of a simple, real-time, cost effective and non-invasive technique for blood microcirculation monitoring. Real-time optical detection and quantification of local haemodynamic parameters may lead to a better understanding of process of angiogenesis and, in turn, to earlier cancer detection, cancer margin delineation, and the monitoring of therapeutic response.

MATERIALS AND METHODS

Experimental Setup

The experimental setup shown in Figure 1a consisted of an OncoLIFE® white light source projected onto tissue via an Olympus BF Type P40® bronchoscope for DR spectroscopy illumination, and a DOCT probe coupled with a DR collection fiber. The area of illumination for DR was 3 cm^2, while the interrogated area was equal to 0.05 cm^2. The emitted DOCT light had a wavelength of $1{,}300 \pm 30$ nm, while the DR light wavelength resided in the ~430–690 nm spectral band. The DOCT and DR measurements were collected simultaneously.

The DOCT probe was made by splicing a graded-index (GRIN) fiber onto the end of a single mode fiber and then cleaving the GRIN fiber to a length of 450 μm. This length corresponds to a pitch of 0.27 (Fig. 1b). The DR probe consisted of an aluminum-clad fiber polished flat at its end. The two probes were mounted onto a plastic block (G) at a distance and angle that ensured that the DOCT beam was contained within the spectroscopy beam at a working distance of approximately 1 mm. The containment of the DOCT beam within the volume interrogated by the reflectance probe was verified by means of a red laser connected to the DR collection fiber and an infrared DOCT sensor card positioned near the end of the composite probe G. The combined DR/DOCT probe tip holder was mounted onto a galvo-driven motor that oscillated at a frequency of 1 Hz to provide lateral scanning for DOCT imaging. The DOCT images were about 1.8 mm deep, with a lateral dimension that depended on the motor range, but was typically ~2 mm.

Animal Procedure

Several animal models were analyzed [23] and a special bench top animal model was designed for this study. Our in

vivo animal study was conducted on four 150–200 g Lewis male rats (Charles River Laboratories) which were placed on a heating pad under general anaesthesia (2% isoflurane in oxygen). The abdomen was opened and the small intestine was externalized, and carefully stretched flat on a custom-made extendable frame covered with a saline-soaked sponge. Throughout the procedure, the small intestine and sponge periodically received an additional gentle spray of saline to prevent drying. The jejunum was selected for the study, to avoid presence of faeces inside. Data for each rat was collected at three different locations along the jejunum. Care was taken to ensure that the gut tissue was not damaged during the measurement, while immobilization of the tissue minimized the artifacts caused by tissue peristaltic motions, spasms and breathing. Immediately after the last measurement, the rats were euthanized with a barbiturate overdose.

Local Perfusion Control

Four methods were used to change the local perfusion—(1) drug mediated vasoconstriction (VC) (phenylephrine hydrochloride, 100 mM, 5–10 drops topically) and (2) vasodilatation (VD) (papaverin hydrochloride, 500 mM, 20–30 drops topically, both reagents from Sigma–Aldrich), and (3) mechanical occlusion (MO) by applying clamps on both arterial and venous ends and (4) mechanical release (MR).

Doppler OCT Data Processing

High resolution B-mode data was acquired at 1 frame per second on a phase sensitive time domain DOCT system (8 kHz, 512 pixels per A-scan). Doppler information was extracted using a Kasai autocorrelation method on a phase demodulated signal as [11],

$$f_D = \frac{f_s}{2\pi}\tan^{-1} = \frac{\sum_{m=0}^{M-1}\sum_{n=0}^{N-2}[Q(m,n)I(m,n+1) - I(m,n)Q(m,n+1)]}{\sum_{m=0}^{M-1}\sum_{n=0}^{N-2}[I(m,n)I(m,n+I) + Q(m,n)Q(m,n+I)]}, \quad (1)$$

where f_D is the Doppler frequency, I and Q are the in-phase and quadrature components of the demodulated signal, M and N are the size of the window used for averaging in the axial and lateral direction, and f_s is the sampling frequency of 10 MHz with m and n denoting the indices in the depth and lateral directions, respectively. The recorded Doppler frequencies varied from ~100 Hz to over 50 kHz. An aliasing effect, due to fast blood flow, occurred in the form of phase wrapping at 8 kHz increments. Using high-speed techniques, such as those proposed by Morofke et al. [13], the Doppler frequency for each pixel, attributable to flowing blood, was determined through a combination of phase unwrapping and axial Kasai measurements. The Doppler frequency is related to the velocity of the scattering object by,

$$v = f_D \frac{\lambda_o}{2n_t \cos\theta}, \quad (2)$$

where v is the velocity of the scatterer (assumed to be the red blood cells), n_t is the index of refraction, λ_o is the wavelength of the DOCT light source, and is the Doppler angle. In applying this calculation, a region of interest containing Doppler-detected vessels was manually segmented from the B-mode images recording mean Doppler shift and maximum vessel diameter. The measurement reproducibility was better than 20% for all data sets. In this study, acquisition of a reliable measurement for Doppler angle was not feasible, so the determined Doppler frequency was not converted to a velocity as per Eq. (2). However, by comparing the Doppler shift in a given frame with the maximum Doppler shift for the specific data set, a relative velocity can be derived. This has the advantage of removing the unknown Doppler angle and need for index of refraction estimation, while still yielding a meaningful number for the temporal analysis of blood flow parameters. The relative velocity was determined as,

$$v_{rel} = \frac{f_1}{f_{max}} = \frac{\frac{v_1 2n\cos\theta}{\lambda_o}}{\frac{v_{max} 2n\cos\theta}{\lambda_o}} = \frac{v_1}{v_{max}}, \quad (3)$$

where v_{rel} is the relative velocity at a given time, and f_1 and v_1 are the mean Doppler shift and velocity at a given time, while f_{max} and v_{max} are the maximum mean Doppler shift and velocity for the series.

The vessel diameter, based on the presence of Doppler signal, was measured in each of the average velocity frames. In each frame, the maximum vertical diameter of the largest (most representative) vessel was selected. The relative diameter normalized to the maximum diameter in each data set was computed.

Diffuse Reflectance Data Processing

The collected DR spectra were converted in a negative logarithm scale. The heuristic parameter found to be the most sensitive to local blood concentration changes was the sum of the variances above and below the DR spectral slope between 449 and 660 nm. This parameter was conditionally termed the "Blood Supply Index" (BSI). The BSI was computed as,

$$BSI = \left| -\frac{(\lambda_2 - \lambda_1)}{2}((-\log(DR(\lambda_1))) + (-\log(DR(\lambda_2)))) + \int_{\lambda_1}^{\lambda_2} \langle -\log(DR(\lambda))\rangle \partial\lambda \right|, \quad (4)$$

where λ-wavelength, $\lambda_1 = 449$nm and $\lambda_2 = 660$nm, $-\log(DR(\lambda_1))$ and $-\log(DR(\lambda_2))$ are the spectral intensities at 449 and 660 nm respectively.

Blood Supply Index versus blood volume fraction (T_{HB}) and blood oxygenation (SO_2).

Blood Supply Index dependence on blood volume fraction (T_{HB}) and blood oxygenation (SO_2) was found as follows. An in vivo diffuse reflectance spectrum can be modeled by the fitting function as derived in Ref. [17] based on a known expression for the absorption by blood [24–26] as,

$$-\log(\mathrm{DR}(\lambda)) = a + b\lambda + T_{\mathrm{HB}}(\mathrm{SO_2}\mu_a^{\mathrm{HBO_2}}(\lambda) + (1-\mathrm{SO_2})\mu_a^{\mathrm{HB}}(\lambda)) \quad (5)$$

where, $a+b\lambda$ relates to the scattering and tissue absorption (other than blood) background, T_{HB} is the dimensionless blood volume fraction (in% of blood volume per total interrogated volume as derived in Ref. [15]), $SO_2 = HBO_2/HBO_2+HB$ is the blood oxygenation in relative units (range 0–1), $\mu_a^{\mathrm{HBO_2}}(\lambda)$ and $\mu_{ab}^{\mathrm{HB}}(\lambda)$ are absorption coefficients for oxy- and reduced hemoglobin (in cm^{-1}), and HBO_2 and HB are the respective fractions of oxygenated and deoxygenated hemoglobin. Substituting Eq. (5) into Eq. (4) yields,

$$\mathrm{BSI} = \left| \begin{array}{l} -\frac{\lambda_2-\lambda_1}{2}(2a + 1109b + T_{\mathrm{HB}}(\mathrm{SO_2}(\mu_a^{\mathrm{HBO_2}}(449) + \mu_a^{\mathrm{HBO_2}}(660)) + (1-\mathrm{SO_2})(\mu_a^{\mathrm{HBO_2}}(449) + \mu_a^{\mathrm{HBO_2}}(660))))+ \\ +\int_{\lambda_1}^{\lambda_2} \langle a + b\lambda + T_{\mathrm{HB}}(\mathrm{SO_2}\mu_a^{\mathrm{HBO_2}}(\lambda) + (1-\mathrm{SO_2})\mu_a^{\mathrm{HB}}(\lambda))\rangle \partial\lambda \end{array} \right| \quad (6)$$

Eq. (6) can be further simplified by separating the blood absorption parameters as,

$$BSI = \left| \begin{array}{l} \left[-(\lambda_2-\lambda_1)(a+554.5b) + \int_{\lambda_1}^{\lambda_2} \rangle a + b\lambda \langle \partial\lambda \right] + \\ +\left[T_{HB} \left(\begin{array}{l} SO_2 \left(-\left(\frac{\lambda_2-\lambda_1}{2}\left(\mu_a^{HBO_2}(449) + \mu_a^{HBO_2}(660)\right)\right) + \int_{\lambda_1}^{\lambda_2} \rangle \mu_a^{HBO_2}(\lambda) \langle \partial\lambda \right) + \\ +(1-SO_2)\left(-\left(\frac{\lambda_2-\lambda_1}{2}\left(\mu_{ab}^{HB}(449) + \mu_a^{HB}(660)\right)\right) + \int_{\lambda_1}^{\lambda_2} \rangle \mu_a^{HB}(\lambda) \langle \partial\lambda \right) \end{array} \right) \right] \end{array} \right| \quad (7)$$

The first term of the Eq. (7), in square brackets, depicts the contribution of the tissue background absorption and scattering effects. The second term (second and third rows) describes the blood absorption contribution. By isolating the first term one obtains:

$$-(\lambda_2-\lambda_1)(a+554.5b) + \int_{\lambda_1}^{\lambda_2} \langle a + b\lambda \rangle \partial\lambda = 0 \quad (8)$$

Hence, BSI is determined only by the blood absorption (within the framework of the model from Eq. 5). Substituting the values obtained from the tabulated spectra of oxygenated and reduced hemoglobin from Ref. [25] into Eq. (7):

$$\mathrm{BSI} = |T_{\mathrm{HB}}(955\mathrm{SO_2} - 1147)| = T_{\mathrm{HB}}(1147 - 955\mathrm{SO_2}) \quad (9)$$

The model described in Eq. (5) operates only with relative values of fractional volume of blood (T_{HB}, r.u.) which are presented below relatively to its initial value.

In the case of a tumor, the local blood supply condition anticipated is a combination of high hemoglobin concentration [10,27] and low blood oxygenation [28,29]. This should yield a higher value of BSI within the tumor compared to the adjacent normal tissue. For instance in lung tumors, the local blood volume fraction is increased by a factor of 2.3, while blood oxygenation drops from 0.92 to 0.49 [29]. From this we estimate that the BSI will provide a contrast between normal tissue and tumor of 1:5.8. These modeling results indicate the potential of the BSI parameter for malignancy discrimination even if the BSI does not separate the contributions of local blood volume fraction and blood oxygenation.

RESULTS AND DISCUSSION

Results of the DR-DOCT correlative experiment are shown on Figure 2. As is visible from DR monitoring in Figure 2a, prior to administration of vasoactive drugs, the baseline data indicative of normal physiologic variation is characterized by a $\sim\pm 20\%$ variability. This deviation is assumed to be a reflection of the animal hart beating and breathing cycles under general anesthesia conditions. Further, the distinct periodic pattern observed within 350–390 seconds and 590–750 seconds intervals is likely related to the local peristaltic motion of the gut.

Once the pharmacological vasoconstrictor was applied, the vessels were observed to constrict almost immediately on DOCT, reaching the lowest level within 80–100 seconds—both in terms of normalized velocity and normalized diameter (Fig. 2b). The DOCT-derived parameters show similar trends throughout all chemically-driven vaso-manipulations in this study. Return to normal local blood supply levels following vasodilator administration were observed to take 150–250 seconds. Vascular changes were observed on DR-derived metrics as well. During vasoconstriction, both the local blood volume fraction and

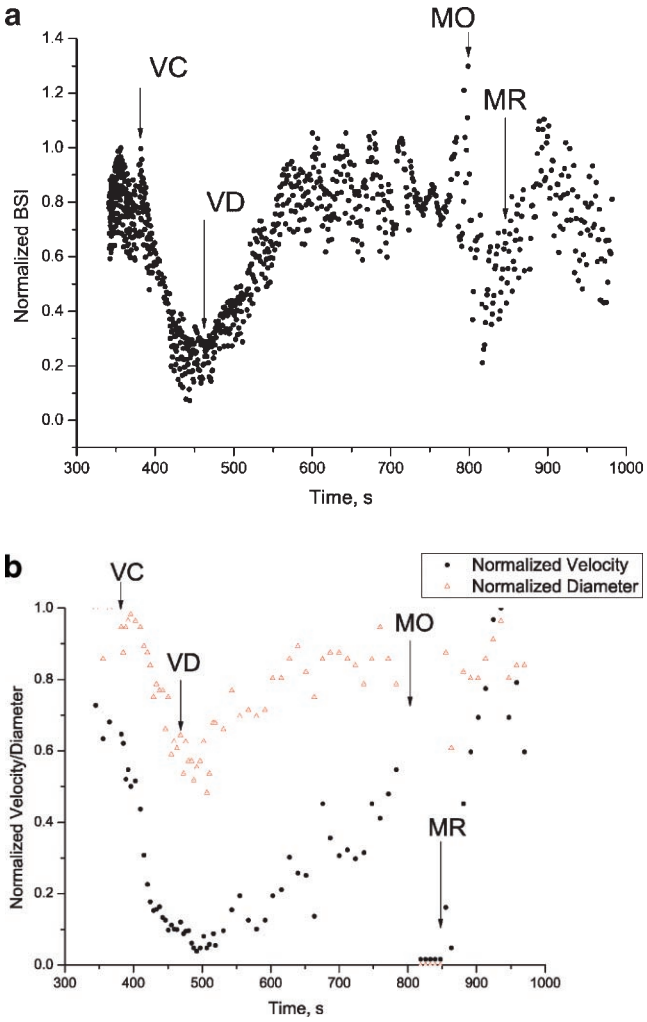

Fig. 2. DR (**a**) and DOCT (**b**) simultaneous monitoring of effects of vasoconstriction (VC), vasodilatation (VD), mechanical vessel occlusion (MO), and mechanical release (MR) [rat #3, spot #3].

blood oxygenation were expected to drop. BSI is directly proportional to the total hemoglobin concentration and inversely proportional to the blood oxygenation, as demonstrated in Eq. (9). As observed in Figure 2a, this parameter declines over the vasoconstriction phase by a factor of $\sim$6. This significant drop of BSI means that the decrease of the local blood concentration dominates over the blood oxygenation reduction contribution, as these two factors (T_{HB} and SO_2) have opposite effect on BSI. The normalized velocity v_{rel} drops from 0.7 to 0.15 at the vasoconstriction phase and recovers considerably slower than the normalized diameter. Recovery of the vessel diameter D back to 90% of its original level during pharmacologic vasodilatation is mirrored by the BSI parameter dynamics.

Mechanical vessel manipulation through occlusion and release demonstrated a lower DR BSI drop/recovery variations compared to the pharmacologically induced vasoconstriction and vasodilatation with higher data variation ($\pm$50%). This result is particularly noteworthy. During drug-induced vasoconstriction, the affected vessels contain a lower volume of blood and the local perfusion is reduced. During mechanical occlusion, however, the clump was applied both on arterial and venous parts of the blood supply; thus, the deviation of the total amount of blood caused by mechanical occlusion/release is expected to be less, as the blood is 'trapped' but still present. This hypothesis was confirmed through a 10–20% difference in BSI decrease between pharmacologic vasoconstriction and mechanical occlusion being consistently observed throughout this study. Conversely, DOCT-derived parameters are more affected by mechanical manipulations, as the Doppler processing specifically detects moving blood. Thus, the Doppler estimation yielded a null result (within experimental error) in the case of complete mechanical occlusion. Once the vessels were mechanically released, the local perfusion was recovered within 40–60 seconds as revealed by both DR and DOCT parameters.

Further exploration of the relationship between the two monitoring techniques is presented in Figure 3. With the common time variable removed, the parametric plots of the DR parameter versus the two DOCT-derived metrics show pronounced correlations. The linearity of the correlation varies based on the type of vascular manipulation, being strongest for pharmacological vasoconstriction (Fig. 3a). The correlation between DR and DOCT parameters for mechanical effects is shown on Figure 3c,d and starts for normalized BSI range >0.35. It reflects the difference in dynamic range between DOCT and DR parameters as highlighted by the Doppler shift estimation yielding a null result in the case of complete mechanical occlusion while the diffuse reflectance is still measurable. Based on Figure 3c,d, the complete mechanical occlusion occurs within 0.2–0.35 range of BSI.

The DOCT-DR correlations for mechanical occlusions and releases are still evident even after pooling data for the whole experimental data set shown on Figure 4. As seen on these charts, the complete mechanical occlusion was occurring within the $\sim$0.2–0.5 data range of BSI for different investigated spots.

The pharmacologic manipulation results are summarized for the whole experimental data set in Figure 5a,b, showing a significant loss of correlation between DR and DOCT derived parameters. Such a significant correlation loss cannot be caused by the opposite influence of the T_{HB} and SO_2 contributions to the BSI parameter (see Eq. 9). As it was shown on Figures 2 and 3 and discussed above, the T_{HB} influence dominates over the SO_2 contribution for both vasoconstriction and vasodilation manipulations during our study. Instead, the correlation loss may stem from tissue optical property inhomogeneities and resultant deviations between different tissue locations; this supposition is supported by the observation that the correlations between DR and DOCT parameters within a particular spot are significantly higher than those of different spots (compare Figs. 4 and 5).

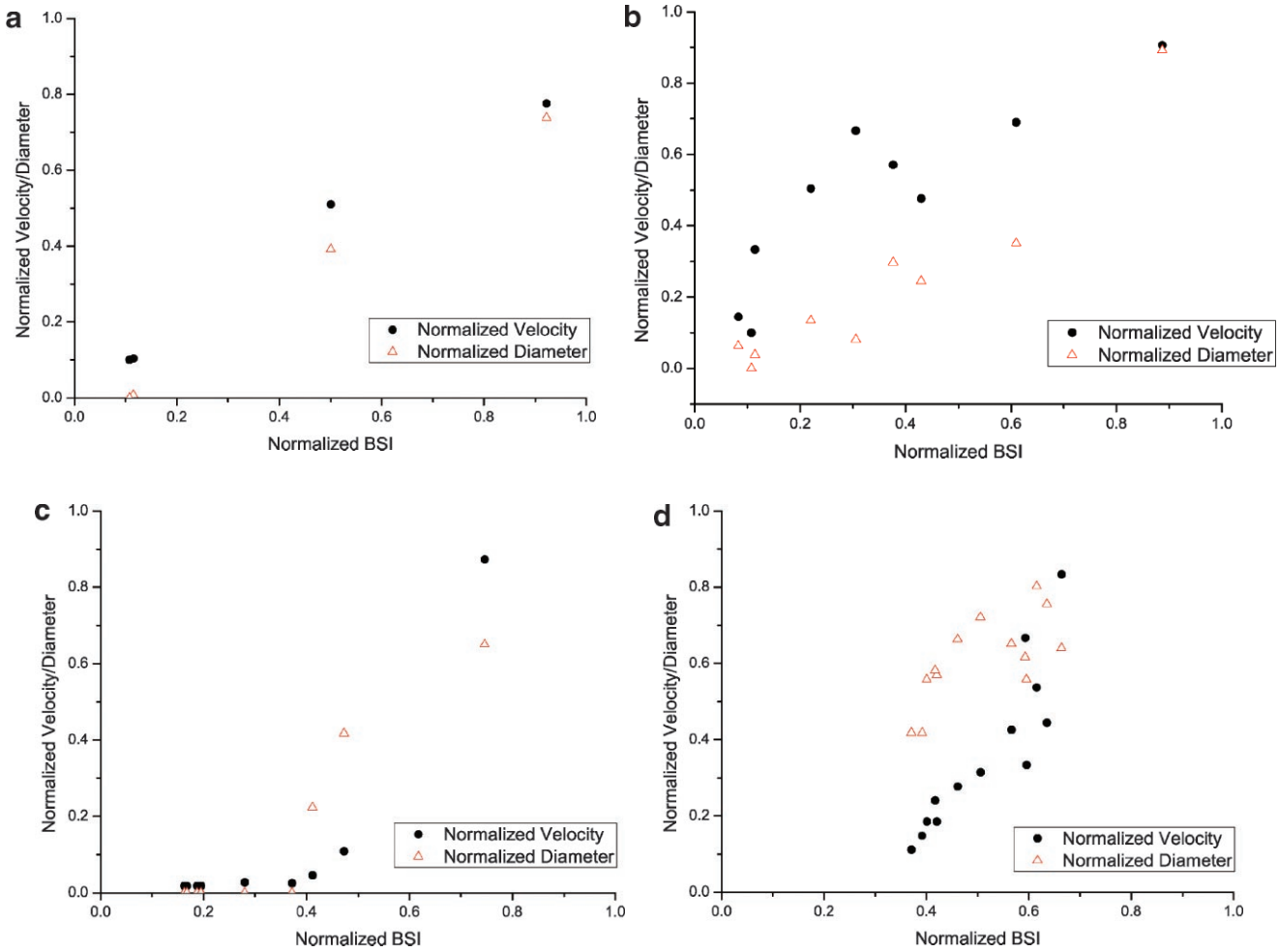

Fig. 3. Examples of the DR-DOCT curves for cases of (**a**) drug-mediated vasoconstriction (VC) [rat #2, spot #2], (**b**) drug-mediated vasodilatation (VD) [rat #2, spot #2], (**c**) mechanical occlusion (MO) [rat #3, spot #3], (**d**) release after mechanical occlusion (MR) [rat #4, spot #3].

The partial correlations seen in Figures 4 and 5 likely stem from the different nature of the two techniques—DR measures local blood volume fraction (volume), whereas DOCT monitors the haemodynamics of moving blood (flow). Another potential source of the correlation reduction is a mismatch of the sampling volumes between the both methods due to the geometrical and wavelength differences, although these are difficult to quantify.

Overall we conclude that there are several non-unique and partially related descriptors/metrics of local tissue haemodynamics all reporting on slightly different aspect of the underlying tissue function/physiology. Furthermore, the optical properties of tissue, such as intrinsic tissue scattering and absorption (beyond blood absorption), vary between the investigated spots and during vaso-manipulations, and these variations can significantly affect the DR results and DR-DOCT interdependencies. This may explain the observation that the correlations between DR and DOCT parameters within a particular spot are significantly higher than those of different spots as comparing Figure 4 versus Figure 5. We assume that normalizing BSI can reduce the DR inter-spot data deviation by the diffuse reflectance integral over the 630–690 nm band, where the blood absorption is minimal for normal (60–95%) values of SO_2 [30]. Oxyhemoglobin absorption is 8–10 times lower than that of reduced hemoglobin for this range [25]. Such normalization of the DR data and exploration of other DOCT-derivable metrics are currently being investigated in our laboratory.

SUMMARY AND CONCLUSIONS

A consistent and reproducible correlation was found between DR and DOCT parameters collected during pharmacologically and mechanically induced vasoconstriction and vasodilatation in a rat gut model. A simple heuristic real time DR spectroscopy metric, the Blood Supply Index, was derived from the data to estimate the local blood supply in vivo. Its behavior in response to vaso-manipulations showed reasonable correlation with average blood flow as quantified by DOCT.

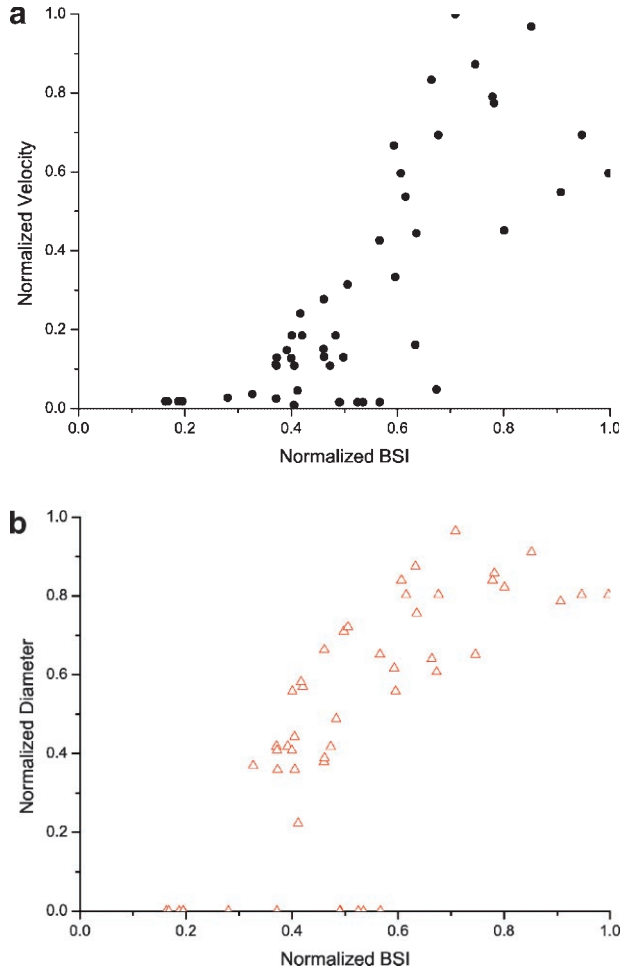

Fig. 4. BSI versus DOCT-derived (**a**) blood flow velocity [data collected from 2 rats, 3 spots] and (**b**) blood vessel diameter [data collected from 2 rats, 3 spots] during mechanical occlusion and release (MO-MR).

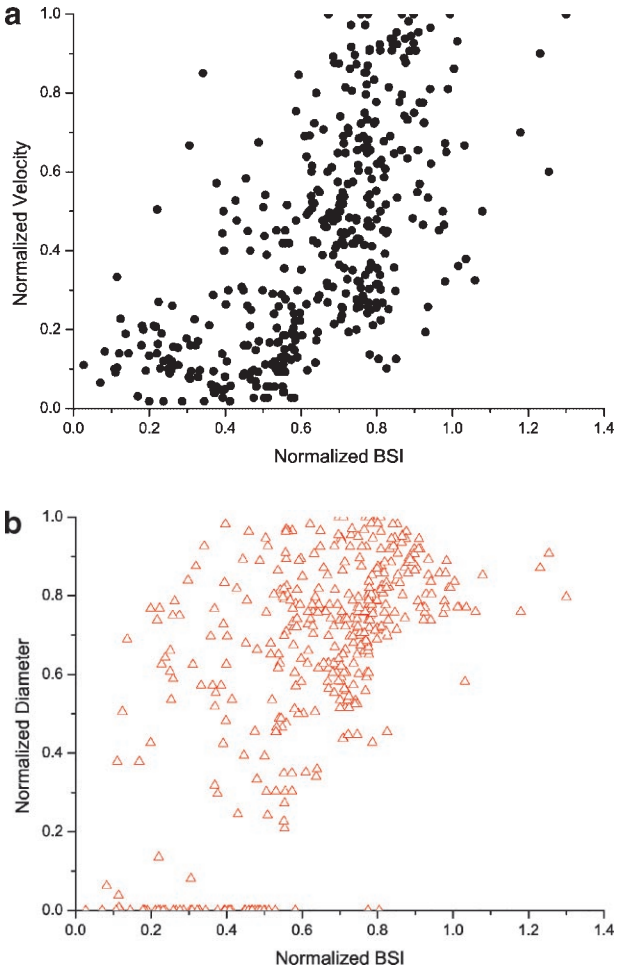

Fig. 5. BSI versus DOCT derived (**a**) blood flow velocity [data collected from 4 rats, 8 spots] and (**b**) blood vessel diameter [data collected from 4 rats, 8 spots] during pharmacologic vasoconstriction and vasodilatation (VC-VD).

However, a significant loss of the correlation between the DR and DOCT parameters is discovered when data from different tissue spot were summarized. We assume that this loss takes place not because BSI cannot distinguish changes in oxygen saturation from changes in local blood volume fraction but rather stem from tissue optical property peculiarities and thus data deviations between different tissue spots.

The presented DR and DOCT methodologies are currently being pursued in our lab for a variety of preclinical and clinical studies, including earlier cancer detection based on local blood supply measurements. The utility of a combined DR-DOCT approach lies in its ability to resolve slightly different (and potentially complementary) aspects of blood supply in tumors, leading to a better understanding of the underlying pathomorphological, physiological and functional intricacies of malignant sites at different stages of cancer development related to tumor angiogenesis and blood supply. A more reliable cancer diagnostic approach may thus emerge from a hybrid measurement approach.

In the near future, the diffuse reflectance spectroscopy will be converted into spectral imaging system that can facilitate a large field of view screening, revealing loci with anomaly local blood supply that may reflect cancerous transformation [31] as a potential guidance for the DOCT optical biopsy.

ACKNOWLEDGMENTS

This study was supported by Ontario Research and Development Challenge Fund (ORDCF), Canadian Institutes for Health Research (CIHR), Photonics Research Ontario (PRO) and Xillix Technologies Corporation (Richmond, British Columbia, Canada). The authors would like to thank Professor Lothar Lilge and Dr. Eduardo Moriyama, Dr. Margarete Atkins, Dr. Max Loshchenov,

Dr. Stuart Bisland and PhD student Beau A. Standish of the Ontario Cancer Institute for valuable experimental help and insightful suggestions.

REFERENCES

1. Carmeliet P, Jain R. Angiogenesis in cancer and other diseases. Nature 2000;407:249–257.
2. Hafstrom L, Persson B, Sundqvist K. Influence of vasoactive drugs on blood flow in subcutaneous tumors—An experimental study in rats. J Surg Oncol 1980;14(4):359–366.
3. Fenton B, Paoni S. Oxygenation and vascular perfusions in spontaneous and transplanted tumor model. Oxygen Transport to Tissue XXIV. Adv Exp Med Biol 2003;530:165–176.
4. Alcázar JL. TI: Tumor angiogenesis assessed by three-dimensional power Doppler ultrasound in early, advanced and metastatic ovarian cancer: A preliminary study. Ultrasound Obstet Gynecol 2006;28–3:325–329.
5. Schilling MK, Redaelli C, Friess H, Blum B, Signer C, Maurer CA, Büchler MW. Evaluation of laser Doppler flowmetry for the study of benign and malignant gastric blood flow in vivo. Gut 1999;45:341–345.
6. Anderson CM. GI magnetic resonance angiography. Gastrointest Endosc 2002;55 (7 Suppl) S42–S48.
7. Li J, Dietsche G, Iftime D, Skipetrov S, Maret G, Elbert T, Rockstroh B, Gisler T. Non-invasive detection of functional brain activity with near-infrared diffusing-wave spectroscopy. J Biomed Opt 2005;10:044002-1-12.
8. Meglinski I, Korolevich A, Tuchin V. Investigation of blood flow microcirculation by diffusing wave spectroscopy. Crit Rev Biomed Eng 2001;29(N3):535–548.
9. Guo L, Burke P, Lo SH, Gandour Edwards R, Lau D. Quantitative analysis of angiogenesis using confocal laser scanning microscopy. Angiogenesis 2001;4(3):187–191.
10. Hidovic-Rowe D, Claridge E. Modeling and validation of spectral reflectance for the colon. Phys Med Biol 2005;50: 1071–1093.
11. Yang VXD, Gordon ML, Qi B, Pekar J, Lo S, Seng-Yue E, Mok A, Wilson BC, Vitkin IA. High speed, wide velocity dynamic range Doppler optical coherence tomography (Part I): System design, signal processing, and performance. Optics Express 2003;11(N7):794–809.
12. Yang VXD, Tang S, Gordon ML, Qi B, Gardiner G, Cirocco M, Kortan P, Haber GB, Kandel G, Vitkin IA, Wilson BC, Marcon N. Endoscopic Doppler optical coherence tomography in the human GI tract: Initial experience. Gastrointest Endosc 2005;61(N7):879–890.
13. Morofke D, Kolios M, Vitkin IA, Yang V. Wide dynamic range detection of bi-directional flow in Doppler OCT using 2-dimensional Kasai estimator. Optics Lett 2007;32:253–255.
14. Duck FA. Physical properties of tissue: A comprehensive reference book. Academic Press; London, UK: 1990.
15. Dymling SO, Persson HW, Hertz CH. Measurement of blood perfusion in tissue using doppler ultrasound. Ultrasound Med Biol 1991;17:433–444.
16. Toyota Y, Honda H, Omoya T, Inayama K, Suzuki M, Kubo K, Nakasono M, Muguruma N, Okamura S, Shimuzu I, Ii K, Ito S. Usefulness of a hemoglobin index determined by electronic endoscopy in the diagnosis of Helicobacter Pylori gastritis. Dig Endosc 2002;14:156–162.
17. Stratonnikov A, Loschenov V. Evaluation of blood oxygen saturation in vivo from diffuse reflectance spectra. J Biomed Opt 2001;6(4):457–467.
18. Gebhart S, Mahadevan-Jansen A, Lin W. Experimental and simulated angular profiles of fluorescence and diffuse reflectance emission from turbid media. Appl Opt 2005; 4(N23):4884–4901.
19. Douplik A, Marcon NE, Cirocco M, Basset N, Streutker C, Zanati SA, Cho S, Wilson B. Reflectance spectroscopy clinical study of dysplastic versus nondysplastic contrast in terms of total hemoglobin and oxygenation in patients with Barrett Esophagus. Gastroenterology (in press).
20. Yang V, Vitkin IA. Principles of Doppler optical coherence tomography. Regar E, van Leeuwen T, Serruys P, editors. In Handbook of Optical coherence tomography in cardiology. Taylor and Francis Medical; Oxford, UK: 2006. Chapter 32.
21. Yang VXD, Mao L, Munce N, Standish B, Marcon NE, Kucharczyk W, Wilson BC, Vitkin IA. Interstitial doppler optical coherence tomography. Optics Lett 2005;30:1791–1793.
22. Yang VXD, Gordon ML, Tang S, Marcon NE, Gardiner G, Qi B, Bisland S, Seng-Yue E, Lo S, Pekar J, Mok A, Wilson BC, Vitkin IA. High speed, wide velocity dynamic range Doppler optical coherence tomography (Part II): In vivo endoscopic imaging of blood flow in the rat and human gastrointestinal tracts. Optics Express 2003;11(N):2416–2424.
23. Galanzha EI, Tuchin VV, Zharov VP. Advances in small animal mesentery models for in vivo flow cytometry, dynamic microscopy, and drug screening (invited review). World J Gastroenterol 2007;13(2):198–224.
24. Jacques SL. 1998; Skin Optics (Portland, OR: Oregon Medical Laser Centre) 1998; http://omlc.ogi.edu/news/jan98/skinoptics.html.
25. Prahl SA. 1999; Optical Absorption of Hemoglobin (Portland, OR: Oregon Medical Laser Centre) 1999; http://omlc.ogi.edu/spectra/hemoglobin/index.html.
26. Meglinski IV, Matcher SJ. Quantitative assessment of skin layers absorption and skin reflectance spectra simulation in the visible and near-infrared spectral regions. Physiol Meas 2002;23:741–753.
27. Zonios G, Perelman LT, Backman V, Manoharan R, Fitzmaurice M, Van Dam J, Feld MS. Diffuse reflectance spectroscopy of human adenomatous colon polyps in vivo. Appl Opt 1999;38:6628–6637.
28. Höckel M, Vaupel P. Tumor hypoxia: Definitions and current clinical biologic and molecular aspects. J Natl Cancer Inst 2001;93:266–276.
29. Amelink A, Sterenborg H, Bard M, Burgers S. In vivo measurement of the local optical properties of tissue by use of differential path-length spectroscopy. Opt Lett 2004;29: 1087–1089.
30. Tsai A, Johnson P, Intaglietta M. Oxygen gradients in the microcirculation. Physiol Rev 2003;83:933–963.
31. Tromberg BJ, Shah N, Lanning R, Cerussi A, Espinoza J, Pham T, Svaasand L, Butler J. Non-invasive in vivo characterization of breast tumors using photon migration spectroscopy. Neoplasia 2000;2(1–2):26–40.